Optical Amplifier for Space Applications

Richard L. Fork, Spencer T. Cole, Lisa J. Gamble, William M. Diffey,
Department of Electrical and Computer Engineering
University of Alabama in Huntsville, Huntsville, Alabama 35899
fork@ece.uah.edu

Andrew S. Keys
NASA-Marshall Space Flight Center, Huntsville, Alabama 35812

Abstract: We describe an optical amplifier designed to amplify a spatially sampled component of an optical wavefront to kilowatt average power. The goal is means for implementing a strategy of spatially segmenting a large aperture wavefront, amplifying the individual segments, maintaining the phase coherence of the segments by active means, and imaging the resultant amplified coherent field. Applications of interest are the transmission of space solar power over multi-megameter distances, as to distant spacecraft, or to remote sites with no preexisting power grid.

OCIS codes: (140.3280) Laser amplifiers; (140.3290) Laser arrays

References and Links

1. J. Mankins, "A Fresh Look at Space Solar Power: New Architectures, Concepts and Technologies", http://www.tier.net/sunsat/freshlook2.htm, October 6 (1997).
2. J. Mankins and J. Howell, "An Executive Summary of Recent Space Solar Power Studies and Findings", NASA Space Solar Power Exploratory Research & Technology (SERT), April 23 (1999).
3. R.L. Fork, C.V. Shank, and R.T. Yen, "Amplification of 70-fs optical pulses to gigawatt powers," Appl. Phys. Lett. **41**, 223-225, (1982).
4. A. Giesen, H. Hügel, A. Voss, K. Wittig, U. Brauch, H. Opower, "Scalable Concept for Diode-Pumped High- Power Solid-State Lasers", Applied Physics **B58**, 365-72 (1994).
5. A. Giesen, private communication.
6. Lisa J. Gamble, William M. Diffey, Spencer T. Cole, Richard L. Fork, and Darryl K. Jones, "Simultaneous measurement of group delay and transmission for a one dimensional photonic crystal", Optics Express **5**, 267-72.
7. See, e.g., A.C.Bordonalli, C. Walton, and Alwyn J. Seeds, "High-Performance Phase Locking of Wide Bandwidth Semiconductor Lasers by Combined Use of Optical Injection Locking and Optical Phase-Lock Loop", Jour. Of Lightwave Technology **17**, 328-42 (1999).
8. John L. Stensby, Phase-Locked Loops: Theory and Application, (CRC Press, New York 1997).
9. Bruce R. Peters, private communication.
10. Herwig Kogelnik, "On the Propagation of Gaussian Beams of Light Through Lenslike Media Including those with a Loss or Gain Variation", Appl. Opt. **4**, 1562-69 (1965).
11. Lee Casperson and Amnon Yariv, "The Gaussian Mode in Optical Resonators with a Radial Gain Profile", Appl. Phys. Lett. **12**, 355-357 (1968).
12. J. W. Goodman, Introduction to Fourier Optics, (McGraw-Hill, New York 1988)
13. See, e.g., Micro-optics: elements, systems, and applications, H.P. Herzig, ed. (Taylor and Francis, London, 1997), especially, J. R. Leger, "Laser Beam Shaping".
14. Hönninger, I. Johannsen, M. Moser, G. Zhang, A. Giesen, U. Keller, "Diode-pumped thin-disk Yb:YAG regenerative amplifier", Appl. Phys., **B65**, 423-26 (1997).
15. U. Roth, Thomas Graf, E. Rochat, K. Haroud, Jürg E. Balmer, and Heinz P. Weber, "Saturation, gain, and Noise Properties of a Multipass Diode-Laser-Pumped Nd:YAG CW Amplifier", IEEE J. Quantum Electron. **34**, 1987-1991 (1998).
16. John Nees, Subrat Biswal, Frédéric Druon, Jérôme Faure, Mark Nantel, Gérard A. Mourou, Akihiko Nishimura, Hiroshi Takuma, Jiro Itatani, Jean-Christophe Chanteloup, and Clemens Hönninger, "Ensuring Compactness, Reliability, and Scalability for the Next Generation of High-Field Lasers", IEEE Selected Topics in Quant. Electron. **4**, 376-384 (1998).
17. Andrew S. Keys, Spencer T. Cole, Richard L. Fork, "Open Multipass Amplifier Quicktime Movie", http://www.uah.edu/LSEG/amp-mov.htm, (1999).

1. Introduction

Technical arguments have been advanced that space solar power systems producing gigawatts of continuous power could be realized within the next decade [1,2]. This possibility

recommends attention to safe transmission of large average power by optical means over the multi-megameter distances encountered in space applications. The reduced diffractive spreading strongly favors optical fields over microwave fields for megameter and longer distances. The amplification of optical fields to high power with good phase coherence over the large apertures needed for efficient transmission has, however, proven difficult to achieve. We suggest that the difficulty can be traced, in part, to a basic conflict between the design rules for optical apertures in space and the design rules for optical high gain amplifiers.

The design rules for large optical apertures in space favor disk-like shapes. The propagation distances of multi-megameters require aperture dimensions of the order of ten meters, or more, for efficient transmission. The need to keep mass low favors a thin structure. Furthermore, practical constraints on the size of objects that can be transported to space favor segmentation of the components that constitute the aperture.

The design rules for high gain optical amplifiers favor a long rod-like geometry. The gain path is preferably composed of short gain regions separated by long regions having no gain. The long rod-like path provides large net gain in the forward direction, but limits gain in the transverse direction. This is minimizes loss to parasitic oscillations and unwanted super-radiance in the transverse direction. The rod-like geometry and the discrete axially segmented nature of the gain regions also assist in limiting gain depletion by amplified spontaneous emission along the amplifier axis [3].

There are additional rules that further complicate the design task. The need to remove heat rapidly with minimum stress on the amplifying material favors a thin disk active medium in good contact with a heat sink over the disk surface [4]. An orientation of the plane of the thin disk normal to the direction of propagation is also desirable as a means of minimizing distortion by thermally induced gradients in the refractive index. Thin disk based laser oscillators using Yb^{3+} doped solid state hosts that meet these requirements have been pioneered by Giesen and coworkers. Those authors report impressive optical to optical efficiencies (e.g., >60%) and amplified wavefronts having low phase distortion despite optical field intensities that approximate the saturation fluence, $10kW/cm^2$, for Yb^{3+} doped materials [4,5]. These thin disks, however, have a short amplifying path, ~200 microns and the transverse dimension for efficient amplification is <1 cm [5].

2. Spatial segmentation strategy

We suggest a strategy for amplification to high average power with good phase coherence over large apertures despite these complex and often conflicting design rules. Our strategy which, as we discuss below will be demanding to implement, involves four steps. The first task is to form a reference optical field that may either be generated at the transmitting site or sent from the site to receive the transmitted power. The second task is to sample the reference optical field with the samples taken sufficiently closely that the optical phase variation measured from sample to sample transversely across the wavefront is very small compared to pi. The third is amplify to high average power each of the sampled segments in combination with active monitoring and maintenance of the phase properties of each spatially resolved optical field component relative to the original reference wavefront. The fourth step is a coherent recombining of the spatially resolved, but amplified and phase coherent, beams to form a high average power coherent optical field to be transmitted to the receiving site.

We suggest that recent advances in rapid measurement of optical phase distortion [6], improving phase lock loop control [7,8], advances in manufacturing of space optics [9] and advances in related areas allow serious consideration of this demanding, information intensive, control strategy. This strategy is primarily relevant to applications in space. Unlike terrestrial applications, optical wavefronts in space tend to have a long spatial period for the transverse optical phase. For example, the spatial period of the transverse phase for a spherical optical wavefront of one-micron wavelength and a radius of a megameter is approximately one meter. This provides an opportunity to introduce a compact high gain high average power amplifier with transverse dimensions that are small compared to the transverse period of the optical phase. In effect we seek to amplify the wavefront on a fine enough scale so that no

important transverse phase information is lost. An array of such amplifiers provides a means of achieving the needed high gain and high average power. We describe in this current paper a design for an open multipass amplifier that is especially compact and that offers a path that could resolve a number of the above conflicting design rules. We also seek features in the amplifier design that will assist in the demanding task of maintaining phase coherence.

We consider the case where the individually sampled and amplified optical fields evolve during amplification to a Gaussian distribution. This is a typical spatial distribution for an amplified field of arbitrary initial spatial distribution that has propagated through a high gain amplifier where the amplifier provides a gain region of cylindrical symmetry and an approximately quadratic decrease of the gain normal to the propagation axis. Kogelnik has provided a calculation characterizing this behavior [10]. Casperson and Yariv have demonstrated the behavior experimentally [11]. Since our amplifier is optical pumped and has approximate axial symmetry, we expect to be able to approximate these conditions in practice well enough to make the Gaussian assumption relevant. We further regard these fields as apertured by a circular boundary of diameter d, but also assume d is sufficiently large compared to the radius of the Gaussian beam, ω_o, that we can neglect the clipping effects of the aperture on the beam.

We also provide for illustrative purposes a numerical example. We choose ω_o = 1.5 mm and d = 6 mm. We further assume that we have used the control of the phase of the individual optical fields to give the array of optical fields a phase curvature over the array of $\exp -j\left(x^2+y^2\right)/\lambda z_o$ where z_o is the distance from the emitting plane to the receiving site, ~36 Mm for our example. The aperture dimension we take as D, ~ 10 m. This is a dimension approximating the diameter of the large optics intended for next generation telescopes in space. The phase variation over the wavefront of an individual Gaussian mode centered at location x, y due to this term is consequently very small. We regard these Gaussian fields as having a beam waist at the emitting plane and consequently treat the phase as flat over transverse dimensions of order d with the phase being assigned the value of $\left(x^2+y^2\right)/\lambda z_o$ at the midpoint of the mode. The field at the emitter plane (z=0) is

$$E_s(x,y) = E_{so}\left[\exp-\left(x^2+y^2\right)/\omega_o^2\right] * \left[\mathrm{comb}(x/X)\mathrm{comb}(y/Y)\right] \left[\mathrm{Rect}(x/D)\mathrm{Rect}(y/D)\right]\exp-j\left(x^2+y^2\right)/\lambda z_o \quad (1)$$

Representative parameter values are z_o =36 Mm, D= 10 m, X=Y=6.8 cm, d= 6 mm, ω_o=1.5 mm and λ = 1 micron. The origin is taken at the center of the emitter. A schematic diagram of the optical field produced by such an array as viewed along the z axis, looking toward the origin from positive z, is shown below in Fig. 1.

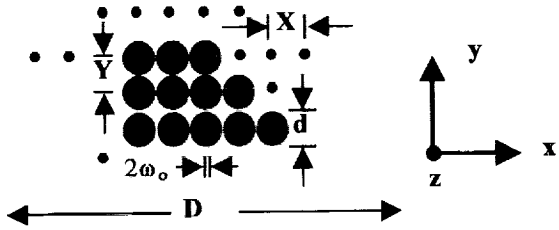

Fig. 1. Cross section of the optical field as viewed looking along z toward the origin.

The point of giving the mean wavefront over the large segmented aperture a phase curvature $\left(x^2+y^2\right)/\lambda z_o$ is that the focal plane for the emitted radiation will be located at z_o. The Fraunhofer approximation consequently applies. We can thus determine the optical field at the receiving site as the Fourier transform of the field at the emitting site. Using the well known properties of Fourier transforms we have for the field at the receiving site, aside from a phase factor that is unimportant given the assumption we are only interested in the received intensity

$$E_r\left(x,y,z=z_o\right)=E_{ro}\exp-\left[\left(\pi\omega_o\right)^2\left(x^2+y^2\right)/\left(\lambda z_o\right)^2\right]\left[\mathrm{comb}\left(xX/\lambda z_o\right)\right] \quad (2)$$
$$\left[\mathrm{comb}\left(yY/\lambda z_o\right)\right]*\left[\mathrm{sinc}\left(xD/\lambda z_o\right)\mathrm{sinc}\left(yD/\lambda z_o\right)\right]$$

A rich variety of alternative distributions could also be realized by varying the structure of the emitter and the phase and intensity profiles. The principal point to be made here is that, assuming λ and z_o are given, we can produce through the choice of the parameters, D, X, Y, and ω_o a specifically structured spatial distribution at the receiving site. There will be localized areas having dimensions of the order of $\lambda z_o/D$ separated by distances of $\lambda z_o/X$ and $\lambda z_o/Y$. The overall distribution will have dimensions of the order of $\lambda z_o/\pi\omega_o$. These can dimensions can be useful for many applications. Specific numerical values for these parameters are given in the conclusion section.

3. Open Multipass Optical Amplifier

Given the above arguments that a spatially segmented coherent emitter could be useful for power beaming, we have designed an open multipass optical amplifier offering high gain, high average power, and compact geometry. We include an incremental amplification process that lends itself to minimization of phase distortion and high beam quality. In particular, we require an amplifier transverse dimension very small compared to one meter. We also require a structure, Fig.2, that permits frequent monitoring of the beam during the amplification and

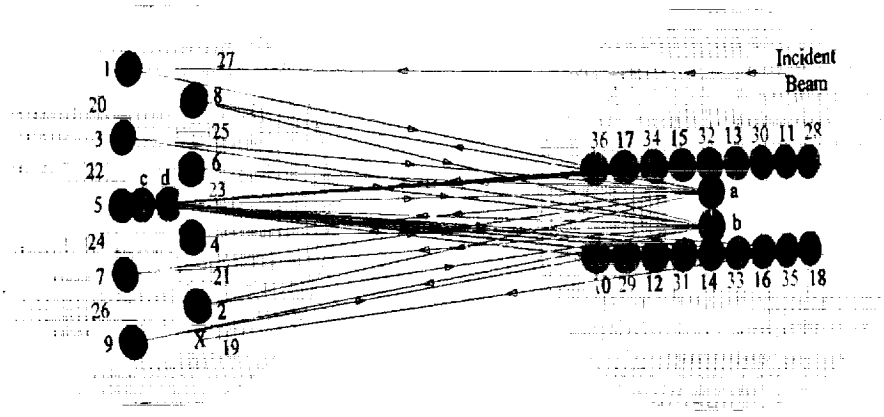

Figure 2: The first 16 paths of the amplified beam (red) are shown. The second 16 passes of the amplified beam, the reflectors for the pump beams, and the pump beams are not shown. The complete set of 36 locally configured reflecting regions (black, yellow, light blue, green) that determine the beam path are shown. The complete set of four active thin disk mirrors (deep blue), one pair on each the two semi-transparent (gray) concentric spherical construction surfaces, are shown. The view on the right is through the back of the semi-transparent construction surface (gray). We denote the array on the left *L* and the array on the right *R*.

frequent opportunity for correction of the various orders of phase distortion. We have chosen to design this amplifier in terms of thin disk active mirrors. The particular design challenge encountered here is one of folding a very long segmented amplifier path within a small volume. The intent is to use this compact amplifier as a modular element in a disk shaped optical emitter of multi-meter transverse dimensions. We need to include in this compact geometry some 54 different reflecting surfaces each having a unique orientation so as to support a continuous optical path. There appears to be no simple conventional optical surfaces that can meet this need.

We address this problem by relying on emerging fabrication techniques for space optics that offer the possibility of optical structures that embed a complex array of specifically articulated individual structures in a larger structure so as to achieve a monolithic, but complex optical surface. We do not detail here the fabrication methods, but do note that current exploratory research on space optics performed by Plasma Processes, Inc., originally addressing x-ray telescopes, demonstrates that individual inserts with unique surface geometries can be individually processed and then fit into a larger structure. The result is to integrate optical surfaces with differing geometries into a single monolithic structure. This provides both robustness and an opportunity to design the complex type of monolithic optical surface that forms the basis of our amplifier.

Given this option we have used the sophisticated software package ASAP (Advanced Systems Analysis Program) to develop the ray trace diagram, Fig.s 2-5, for a 64 pass (32 pump and 32 probe) system. This optical system provides the 64 passes in a compact structure that, given the fabrication techniques identified above, has the robust character of a monolithic structure and a compact volume.

4. Beam path geometry

We illustrate the particular beam path geometry for this compact densely packed array of beam paths in more detail in Fig. 3. A key to realizing this geometry is the use of two pairs of thin disk active mirrors with each pair located centrally on each of two opposing arrays of reflectors. The disks and the reflector arrays are best understood in terms of their location on

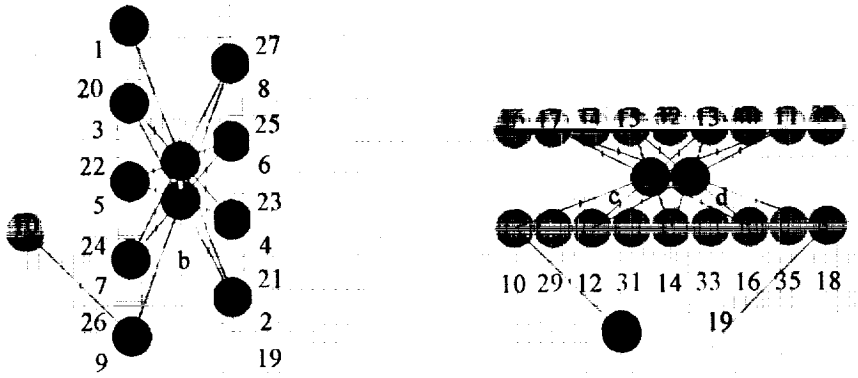

Figure 3. Schematic of the beam routing for the first 16 amplified beam passes. The nine reflectors (1-9 shown in black) guide the first eight passes. These reflectors are located on the left array in Fig. 2. The two thin disks accessed during these 8 passes (a, b shown in deep blue) are physically located on the right array in Fig. 2. The next eight passes are guided by the nine reflectors on the right array in Fig. 2 (10-18 shown in green). These experience gain on reflections from the thin disk pair (c, d shown in deep blue) on the left array as viewed in Fig. 2. The linking steps 9-10 and 18-19 are indicated. The view is as seen looking along the system axis from right to left in Fig. 2.

two concentric spherical surfaces (indicated in the figure in gray). These surfaces are used here as construction surfaces that assist in this discussion. These are not actual physical surfaces, but rather approximate the mean surfaces of the arrays. We include these surfaces to assist in discussing the orientation and location of the thin disks and the various local reflecting regions.

The two disks on each surface are necessary to the particular pattern of reflections we use. The beam alternates between two disks on a given reflector array on successive bounces. This is essential to creation of the stepping pattern that progressively explores the surfaces of the two reflecting arrays. A second feature is that each of the reflecting surfaces is designed to be approximately flat despite being located on a spherical construction surface. Some small optical power could be useful in some applications for maintaining or progressively modifying beam diameter. The approximately flat character is useful in providing both redirection of the beam and at the same time maintaining the relatively large beam diameter at the thin disks needed for efficient and large power extraction from the active mirror element.

A third distinctive feature is that while 28 of the reflecting regions have their surfaces tangent to the spherical construction surface, 8 of the 36 local reflecting regions depart slightly from such a tangent condition. These departures in orientation are essential in allowing the continuous 12.8 m beam trajectory that would not be possible with a simpler surface. These departures are also helpful in the introduction and extraction of the beam while avoiding any need for active switching in and out as in conventional regenerative amplifiers.

We have examined several physical optics aspects of the beam propagation through the amplifier. In particular, we use reflecting regions having a 6 mm diameter which is sufficiently large compared to the 1.5 mm beam radius to avoid significant clipping of a well aligned beam. We have also examined depolarization issues. Since the beam path involves only reflections near normal incidence and all structures have dimensions large compared to the optical wavelength, there is relatively little depolarization under any circumstance. We have performed a simulation using ASAP and modeled reflectors that have a multilayer structure similar to high reflectance dielectric mirrors and also to the photonic band gap structures that we are exploring as a means of active control of higher order phase distortion [6]. We find a worst case net depolarization of the order of 10% for the 32 passes. In general the depolarization can be made less than 1% for the 32 passes by choosing the most favorable polarization of the incident beam.

Each reflection from an active thin disk involves a double pass of the thin disk active medium. A representative double pass gain is 1.25 [4,5]. The thin disk pairs on the two reflector arrays are oriented such that a line drawn between the centers of a disk pair on a given surface is at 90 degrees to the equivalent line for the pair of disks on the opposing surface. This reduces the probability of unintentional laser action occurring due to a direct path between the thin disk active mirrors. This also has the consequence that the sets of the reflectors on the two opposing surfaces are oriented at 90 degrees with respect to each other. We also note the aperture could be more fully filled with reflectors if more passes were needed. The number next to a given reflecting region indicates the nth reflection in the beam trajectory. The reflecting regions for the pump beams and the pump beam paths, not shown in Fig. 3, are shown in Fig. 4.

The amplifier is designed to provide high small signal gain (1262x), to produce a fluence that reaches saturation for the Yb^{3+} host (~10-27 kW/cm^2), and a total average power of ~1 kilowatt. The dimensions are compact (6.8 cm diameter and 20 cm long). This satisfies the constraint identified above that the transverse dimension be small compared to 1 meter. The amplifier length, which is a lower limit on the thickness of a disk shaped aperture formed from a stacked array of these amplifiers, is small compared to the transverse dimensions, ~10m, of large apertures planned for next generation space applications. The optical path is long (12.8 m), of small diameter (3 mm) and segmented (a ~400 micron gain path occurs on each pass through an active mirror and these processes are separated by distances of ~40 cm).

5. Particular local variations in the reflecting surfaces and their purpose

The individual surfaces of reflecting regions 2-8, 11-17, 20-26, 29-35 are tangent to the concentric spherical construction surface at the point where the ray path of the amplified beam intersects the surface of a given reflecting region. Individual surfaces 1,9,10,18,19,27,28, and 36 are rotated slightly off the plane tangent to the construction surface this intersection point so as to redirect the amplified beam in a manner that optimally continues the trajectory of the beam path at the point where the beam reaches one of those reflecting regions. We note that the particular arrangement depicted in Fig.s 2-5 is only one of many forms of this amplifier that could be realized. In general, we expect that a variety of dimensions and reflector patterns will prove useful. Various tradeoffs involving small signal gain, total power, fill factor of the exit aperture, and overall dimensions of the amplifier are clearly accessible.

The pattern of two thin disks per array and the two arrays of reflectors on a given surface serve a function similar to that of right angle mirrors used in the multiple pass resonators for stepping pump beams [4], but does so more economically. Also in a conventional optical system based on simple spherical and simple flat surfaces we would be limited to the first eight passes. After the first 8 passes, the departure from the tangent to the construction surface of reflectors 9 and 10, launches a second pattern of 8 passes. These connecting passes are important in linking the four families of eight passes each. The second family of eight passes walks the beam through the reflectors 10-18 on the second array. The beam is then directed from reflector 18 to reflector 19 (we show this as X in Fig. 2). At this point the beam then executes 16 more passes (not shown in Fig. 2) in a manner similar to the first 16, by using the remaining 18 reflecting regions. The beam then exits from the multipass resonator continuing on in the same general direction as that when it entered the resonator.

6. Optical path sequence

We further detail here the beam paths. The view in Fig. 3 of two reflector arrays is as seen looking along the z-axis from right to left in Fig. 2. The beam paths are structured in the form of four families of passes. Nine reflecting regions (black 1-9, green 10-18, yellow 19-27, and light blue 28-36) guide each successive family of 8 passes. A pass is defined as a beam passing from a given reflecting region to a thin disk on the opposing array, specularly reflecting from the flat mirror backing the thin disk (this involves a double pass through the thin disk active medium) and then returning to the original array of reflectors.

The optical path sequence proceeds 1-a-2-b-3-a-4-b-5-a-6-b-7-a-8-b-9, meaning the beam passes from reflector 1on array ***L*** to thin disk a on array ***R*** to reflector 2 on array ***L***, then to thin disk b on array ***R***, etc. through the remaining reflectors 3-8 and thin disks to reflector 9. The sequence then proceeds 9-10-c-11-d-12-c-13-d-14-c-15-d-16-c-17-d-18. The final sequences are 18-19-b-20-a-21-b-22-a-23-b-24-a-25-b-26-a-27 and 27-28-d-29-c-30-d-31-c-32-d-33-c-34-d-35-c-36. The probe beam then exits from reflector 36 in the same direction as the ray that originally entered the multipass resonator. The orientation of reflector 36 can be varied within reasonable limits to adjust this direction.

Eight of the probe reflectors 1,9,10,18,19,27,28 and 36 serve routing purposes and typically are not tangent to the spherical construction surfaces. The remaining 28 probe reflector regions are tangent to one of the two concentric construction surfaces at the point where the amplified beam intersects the reflector and serve to walk the beam progressively back and forth between the two thin disks near the center of the opposing construction surface. The planes of the thin disks are normal to the axis formed by a line drawn between the centers of the two concentric construction surfaces. The two mirror systems have been rotated at right angles to each other to avoid unintended laser oscillation between directly opposing active thin disks. The confocal parameter for the 3 mm-diameter beam approximates the overall 12.8 m pathlength.

7. Pump beam reflectors and pump beam paths

In addition to the reflectors for the probe beam we also must provide reflectors for the pump beams needed to excite the active thin disk mirrors. The work by Giesen and coworkers has shown that multiple passes are important in achieving the needed pump intensity at the thin disks [4,5]. The pump beam routing is an imaging task different from that for the beam to be amplified. The pump beam is less coherent and requires focusing as well as larger reflecting regions. The pump beam can, however, unlike the beam to be amplified be retroreflected on itself after the first sequence of passes and hence only half as many reflectors are required.

We show the pump beam reflecting regions and a likely set of pump routing paths in Fig. 4. The pump beams are derived, at the time of this writing, from fiber coupled diode bars.

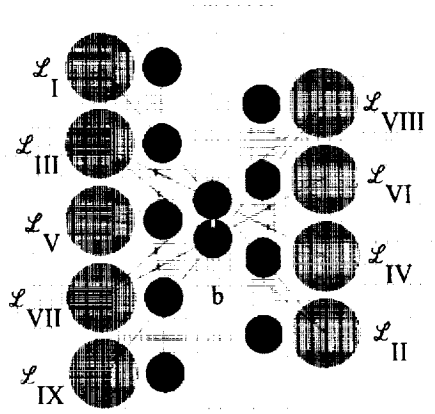

Fig. 4. Pump beam reflectors on the left array (purple $L1$-$L8$) and pump beam paths (green). The pump beam reflectors are larger, and the reflector packing density smaller, as compared to the amplified beam reflectors because of the greater divergence of the pump beam.

The typical pump beam divergence is 12 degrees full angle from a fiber core of ~1.1 mm. The divergence is reducible at the price of a larger beam diameter as allowed by the LaGrange invariance theorem. Reflectors are shown as of 12 mm diameter for this illustrative example. The routing of the pump beams is simpler because of the factor of 2 increase in reflector spacing forced by the larger reflector diameter. One can use one pump beam or two independent pump beams depending on the preferred strategy. The pump reflectors are assumed to be given the particular optical power needed to optimally image the pump beam. The preferred imaging strategy depends on the desired amplified beam diameter and spatial dependence of the pump beam at the thin disks.

8. Combined pump beams, probe beams and reflector systems

The combined pump beams, probe beams, and reflector system are shown in a frame from a QuickTime movie [14] in Fig. 5. The movie is helpful in visualizing and understanding the relatively complex array of reflectors and beams. The 3-D images were developed using ASAP and AutoCAD 2000. This 6.8-cm diameter by 20-cm long amplifier is designed to produce 1 kilowatt of average amplified power in a 3-mm diameter beam. Arrays having a smaller number of probe reflectors can be designed for larger diameter beams, lower gain, and larger fill factor.

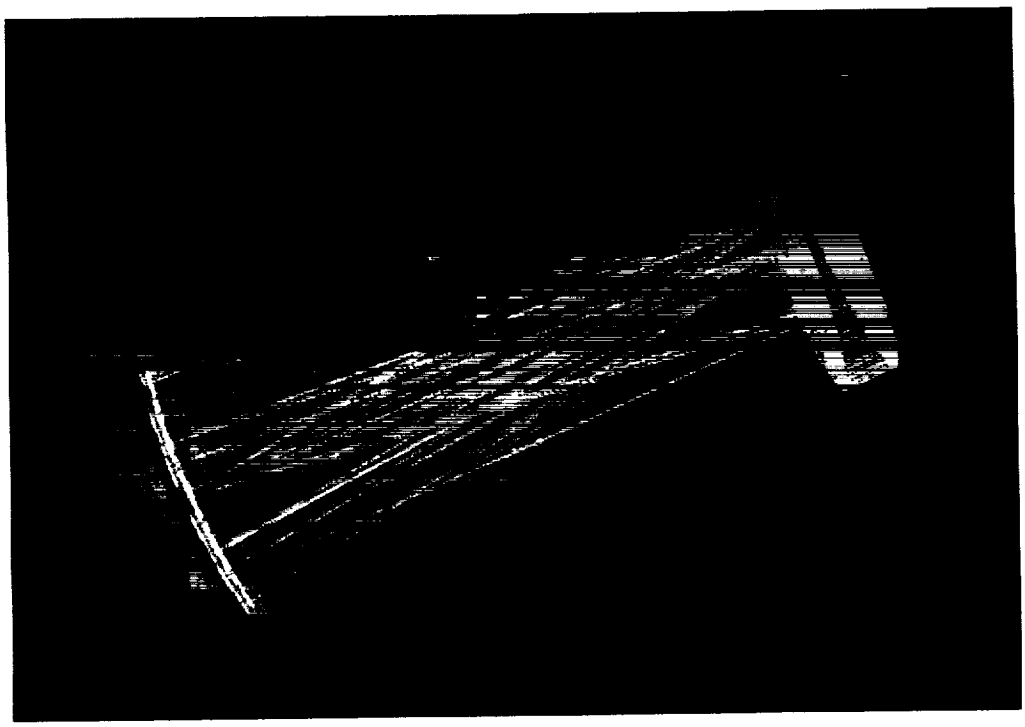

Fig.5. The figure is one frame from a QuickTime movie (2.4 MB). The movie shows the complete reflector system including two pump beams (green and yellow) and the probe (red) beams in 3-D perspective and in rotation. The multiple views from different perspectives provide a useful assist to understanding the beam routing strategy and the reflector configurations.

A natural question emerges concerning the feasibility of coherently combining the multiple amplified coherent beams we discuss here so as to form a single very high intensity beam. Such combining appears possible, in principle, and has been discussed and demonstrated to various degrees at low power levels and for a small number of beams [13]. The main point we make here is that while such coherent combining appears feasible, the optical field manipulation and the additional conventional and non-conventional optics required appears much more complex than the relatively straightforward system we describe here. In particular, the segmented structure with low fill factor we describe above lends itself well to producing a distributed segmented pattern in the far field with precisely localized regions, but not to producing a single concentrated beam.

For the numerical example used here we would have at the far field localized areas of dimension $\lambda z_o / D \sim$ 3.6 m separated by distances of $\lambda z_o / X$ and $\lambda z_o / Y$ of ~529 m. The overall distribution has dimensions of the order of $\lambda z_o / \pi \omega_o$ ~7.6 km. Assuming an average power of 1 kW per amplified component of the field, assuming no transmission losses, this gives 21.63 MW of total average power delivered to ~208 sites at an average power per site of 104 kW per site. The intensity is about 8 kW/m^2 at the receiving site, or about 6 times the intensity of natural sunlight. This could be a useful power source strategy, e.g., for an exploratory expedition to a planetary surface having no preexisting power grid.

9. Related Work

There is relatively little closely related work given the novel optical structure that we address. The use of optical phase loop locking has been recently addressed [7] and the coherent

combining of optical fields has been addressed earlier [13]. None of that work, however, addresses the task of achieving high gain and high average power over large apertures in a spatially segmented, but phase coherent manner. Thin disk regenerative amplifiers based on thin disks containing Yb^{3+} that provide efficient and large multipass incremental gain have been reported [15]. Those regenerative amplifiers require an active switching in, and active switching out, of the signals to be amplified and have not been specifically designed for incorporation into a modular array. A monolithic multipass diode pumped amplifier that has been demonstrated that is designed to have the ruggedness needed for applications in space [16]. That work does not offer high gain to high power or address amplification of optical fields over a large aperture.

We also note that the optical amplifier and imaging strategy we discuss here can be applied to both continuous and pulsed optical fields. As regards pulsed operation a recent review of compact high field lasers provides a measure of the peak intensity using chirped pulse amplification that can be extracted per cm^2 of gain aperture as 10^{23} W/cm^2 for the Yb^{3+} type of system we discuss here [17]. A considerable further effort would be required in our design to achieve approximately unit fill factor and a concentration of the emitted light in a single beam. This does not, however, appear ruled out by either practical or fundamental constraints. We observe that such a system would access the peak intensity, 10^{29} W/cm^2, identified in [17] and references therein, as the threshold for accessing the vacuum nonlinearity.

10. Conclusions

We find a way to reconcile the need for a long segmented rod-like amplifier gain path and a large thin disk-like emitting aperture for high average power. While we have not explored in detail the difficult task of maintaining phase coherence of many optical beams propagating on many physically distinct paths we note that such phase coherence is, and has been, frequently achieved in systems involving smaller numbers of beams [7,13]. We also note that our strategy provides incremental gain steps with frequent opportunity for monitoring and correcting phase distortion. In particular, some of our recently reported experimental work on the use of photonic band gap structures provides a potential means for rapid measurement and correction of higher order phase distortion [6].

Regarding the total optical power that could be transmitted by this method, the key parameters are the total area over which phase coherence can be established, the saturation fluence of the amplifier medium, and the fraction of the aperture filled by the active amplifying medium. The use of fewer reflectors and a larger ratio of beam to amplifier cross section reduces the realizable gain in our system, but increases the fill factor. Multiple stages of amplification with different fill factors would be useful in optimizing output power. As a measure of the total average power achievable in the final amplifier stage if we take the saturation fluence for Yb:silicate of 27 KW/cm^2 and assume a fill factor of 0.1 the total average power for a 10 m dimension aperture is ~2.7 GW. This is of the order of the space solar power [1,2] referenced at the beginning of this article. A segmentation strategy that dispersed this power over a sufficiently large number of sites can be used even with these higher powers to keep the average power at any given site of the order of natural sunlight.

8. Acknowledgments

We thank Bruce Peters and Tim Blackwell for discussions regarding fabrication of space optics, Lloyd Hillman and Dave Lamb for computational facilities, Brian Robinson for discussions regarding the segmented imaging and Wesley Walker for work relating to our website.